Catal Lett (2008) 124:340–351
DOI 10.1007/s10562-008-9473-x

Characterization and Reactivity of TiO_2/SiO_2 Supported Vanadium Oxide Catalysts

Debaprasad Shee · Goutam Deo

Received: 28 January 2008 / Accepted: 12 March 2008 / Published online: 12 April 2008

Abstract Several TiO_2/SiO_2 supports and supported vanadium oxide (vanadia) catalysts of varying titania and vanadia content are synthesized and characterized. Titania rutile phase is not detected for the TiO_2/SiO_2 supports even up to a calcinations temperature of 1073 K. The supported vanadia catalysts were also studied for the ethane and propane ODH reaction and compared with TiO_2 (Degussa P25) supported catalysts. Surface vanadia species are present on the titania or silica part of the TiO_2/SiO_2 support depending on the titania and vanadia loading of the catalyst. Depending on the vanadia loading in the $V_2O_5/TiO_2/SiO_2$ catalyst the anatase to rutile phase transformation may occur below 1073 K. Furthermore, the ODH activity is retained or decreases less rapidly compared to the TiO_2 supported catalyst as the calcination temperature is increased. Consequently, the TiO_2/SiO_2 supported vanadia catalysts do provide certain advantages compared to the TiO_2 (Degussa P25) supported system.

Keywords TiO_2/SiO_2 support · Vanadium oxide · Calcinations temperature · Alkane ODH · Kinetic parameter

1 Introduction

Supported vanadium oxides (vanadia) are used as catalyst for various selective catalytic oxidation processes [1–3]. Of these vanadia supported on titania is considered to be an effective catalyst system. The optimal activity and selectivity of the catalyst is accomplished when the vanadia is dispersed on the anatase phase of TiO_2 [4, 5]. Deactivation with high calcinations temperatures and low surface area of anatase titania are, however, some drawbacks for its use as a catalyst support. For example, it has been reported that for the ODH of propane reaction the propene yield increases with reaction temperature [6]. With an increase in reaction temperature, however, deactivation of the titania supported systems is expected since the catalyst undergoes irreversible changes. Furthermore, it has been observed that creating a higher surface area titania support would help in improving the propene yield since a higher monolayer capacity can be achieved [7]. Thus, it would seem beneficial to synthesis a titania support of relatively high surface area and study the behavior of the catalysts as an effect of increasing calcinations temperature.

One of the methods of achieving a high surface area titania support that is minimally affected by high calcinations temperatures is by using another thermally stable and high surface area oxide support, such as SiO_2 and Al_2O_3, to anchor the titania particle [8, 9] and ref. therein]. For example, previous studies suggest that the anatase phase is stabilized in TiO_2/SiO_2 support at elevated temperature [10]. The dispersion of the surface vanadia phase on these TiO_2/SiO_2 supports is, however, not clear since it has been proposed that the surface vanadia phase may form over the titania or silica part of the support [11, 12]. It would be preferred that the vanadia is present on the more active titania phase since the silica supported vanadia system is a relatively poor catalyst.

The present study attempts to address this issue of creating a support containing high surface area titania on a silica matrix that is thermally stable and can be used to

Electronic supplementary material The online version of this article (doi:10.1007/s10562-008-9473-x) contains supplementary material, which is available to authorized users.

D. Shee · G. Deo (✉)
Department of Chemical Engineering, Indian Institute of Technology Kanpur, Kanpur 208 016, India
e-mail: goutam@iitk.ac.in

support the surface vanadia phase. Though the TiO_2/SiO_2 supported vanadia catalysts have been used for various partial catalytic oxidation and reduction processes [10, 11, 13], the ODH of ethane and propane are chosen as model reactions since previous studies have reported that in these systems supported vanadia catalysts are active and selective [6, 14–17]. Furthermore, the propane ODH reaction is more suitable when the surface vanadia species is dispersed on titania compared to other oxide supports [15, 16]. To the best of our knowledge, a single study exists in the open literature dealing with propane ODH reaction being carried out over a TiO_2/SiO_2 supported vanadia catalysts [18]. This previous study, however does not address the effect of calcination temperature of the catalysts or in detail the effect of vanadia and titania loading on the TiO_2/SiO_2 supported vanadia catalysts. The effect of calcinations temperature on the behavior of the catalyst will be studied by calcining the catalyst at different temperatures prior to obtaining the catalytic data at a specific reaction temperature. Complementary characterization of the catalysts will be obtained. Analysis of the surface active sites will also be carried through kinetic parameters estimated for the propane ODH reaction and the results of the reactivity data will be correlated with the characterization data to provide the structure-reactivity relationship. Comparison with some pure TiO_2 supported catalysts for the propane ODH reaction will also be undertaken.

2 Experimental

2.1 Material Synthesis

A series of TiO_2/SiO_2 supports of varying titania content were synthesized by the incipient wetness impregnation method using a titania precursor on a pretreated SiO_2 support (Aerosil 200). The titania precursor used for the synthesis of the TiO_2/SiO_2 support was titanium ethoxide (Sigma-Aldrich). The pretreatment of SiO_2 was achieved by adding incipient volume of absolute ethanol to SiO_2 followed by drying and heat treatment for which the details can be found elsewhere [6]. During synthesis of the TiO_2/SiO_2 supports incipient volumes of an ethanol solution of titanium ethoxide was intimately mixed with pretreated SiO_2 to make a paste. The paste was kept in a desiccator for drying at room temperature for 8 h and at 383 K for 6 h. The dried TiO_2/SiO_2 supports were finally calcined at 723 K. These support samples were denoted as xTi–Si, where x represents the weight percent of titania as TiO_2. The values of x considered are from 10–70.

The TiO_2/SiO_2 supports containing 30, 50 and 70 wt% of titania as TiO_2, 30Ti–Si, 50Ti–Si and 70Ti–Si, were chosen for the synthesis of supported vanadia catalysts. To understand the effect of vanadia loading, the 50Ti–Si support was considered for the synthesis of the vanadia supported samples containing 2–10 wt% vanadia as V_2O_5. The synthesis of the TiO_2/SiO_2 supported vanadia catalysts was achieved by the incipient wetness impregnation method and the vanadia precursor used was ammonium meta-vanadate (NH_4VO_3). During synthesis the pretreated TiO_2/SiO_2 support was intimately mixed with incipient volume of vanadium oxalate precursor solution to make a paste. The pretreatment of the support are similar to those found elsewhere [6]. The vanadium oxalate precursor solutions were prepared by mixing calculated amounts of ammonium meta-vanadate and oxalic acid in double distilled water. The resulting deep blue solution was diluted to achieve the incipient wetness impregnation volume of the support. The solution was mixed with pretreated TiO_2/SiO_2 support to form a paste. The paste was heat treated similar to the support described above. The catalysts were finally calcined at 723 K. The catalyst samples were denoted as yVxTi–Si, where y is the weight percent of vanadia, as V_2O_5, in the sample. In addition, two catalysts of 2 and 4 wt% vanadia loading as V_2O_5 supported on TiO_2 (Degussa P25) were also considered for comparison purpose. Details of the synthesis of these two samples can be found elsewhere [6]. These samples were denoted as 2VTi and 4VTi.

2.2 Surface Area Measurement

The BET surface area of all the samples was determined by nitrogen absorption method using multipoint BET equation. The samples were degassed by heating the samples at 393 K in flowing helium prior to nitrogen adsorption at 77 K. The apparatus used for these studies was COULTER SA 3100 analyzer equipped with an SA-3100 VIEW™ software package.

2.3 X-ray Diffraction (XRD)

XRD pattern were obtained in the range of 10–70° with a scanning speed of 3° min^{-1} on an ISO Debye flex-2002 X-ray diffractometer using Cu Kα irradiation ($\lambda = 1.54056$ Å).

2.4 Raman Spectroscopy

The Raman spectra of the prepared catalysts under ambient and dehydrated conditioned were obtained using an ultraviolet (UV)-visible Raman spectrometer system (Horbia-Jobin Yvon LabRam-HR) equipped with a confocal microscope, 2400/900 grooves/mm grating and a notch filter. The samples were excited with a 532-nm (Visible) Yag double-diode pumped laser. All the spectra were taken at a resolution of ~ 2 cm^{-1}. For the dehydrated spectra, the

powdered samples were placed in a high temperature in situ cell (Linkam, TS-1500). The samples were pretreated at 673 K in flowing of O_2/He for 0.5 h before the Raman spectra were taken. Additional details are given elsewhere [19].

2.5 Temperature Programmed Reduction (TPR)

Temperature programmed reduction studies of the TiO_2/SiO_2 supported vanadia catalysts were obtained in a Micromeritics Pulse Chemisorb 2705 apparatus loaded with 0.03–0.05 g of samples in a U-tube quartz reactor. Before TPR studies the samples were pretreated in flowing He (30 mL/min) at 473 K for 30 min. The reactor was cooled to room temperature and a 5% H_2–Ar mixture gas at a flow rate of 30 mL/min was introduced into the reactor. The sample was heated to 1200 K temperature using a temperature programmed rate of 10 K/min. Hydrogen consumption was measured by using a thermal conductivity detector.

2.6 Fourier Transform Infrared Spectroscopy (FTIR)

The dehydrated IR spectra of the TiO_2/SiO_2 supports and supported vanadia catalysts were obtained using a BRUKER TENSOR 27 FTIR spectrometer coupled with a diffuse reflectance accessory (HARRICK Praying Mantis, DRP-BR4) and a high temperature reaction chamber (HARRICK HVC-DRP-2) equipped with KBr windows. To obtain the dehydrated IR spectrum the sample cup of reaction chamber was filled with powdered sample and oxygen gas was introduced into the reaction chamber at a flow rate of 15 mL/min. The temperature of the reaction chamber was gradually increased and maintained at 673 K by an automatic temperature controller module (HARRICK ATC-024-2). The spectrum obtained for the samples was subtracted by the spectrum of the pure support using OPUS version 5.5 FTIR data acquisition software (BRUKER). All spectra were recorded against a KBr background and at a resolution of 4 cm^{-1} using a total 16 scans.

2.7 Reaction Studies

The reactivity of the TiO_2/SiO_2 supported vanadia samples were studied for the ethane and propane ODH reaction. For the ODH reactions the conversions, selectivities, yields and kinetic parameters were calculated. The ethane and propane ODH reactions were carried out in a fixed bed, down flow, isothermal tubular quartz reactor at atmospheric pressure. The inlet gas flow rates were controlled by three separate mass flow controllers (Bronkhost Hi-Tech, E1 mass flow controller) for alkane, oxygen and nitrogen. The total inlet gas flow rate was maintained at 75 ml/min for parameter estimation studies and was varied from 30 to 120 mL/min for contact time studies. Contact time studies were performed at 653 K temperature using alkane to oxygen molar ratio 2:1. For kinetic studies involving propane ODH the reaction temperature was varied from 613 to 673 K and propane to oxygen molar ratio was varied from 1:1 to 3:1. Nitrogen was used as a diluent and its quantity was adjusted with oxygen such that the inlet gas composition corresponds to that of air. The alkane conversion for all reactivity studies was maintained below 10% to ensure minimal mass and heat transfer effects. Blank experiments were also carried out at identical reaction conditions to ensure no contribution of homogeneous reaction. Additional details of the reactor setup, calculations for conversion, selectivity and yield can be found elsewhere [6, 7].

2.8 Kinetic Parameter Estimation

The kinetic parameters for the propane ODH reaction are determined using previously described methodologies [7, 20]. An objective function based on the predicted and observed outlet concentrations is used, which is minimized with the help of Genetic Algorithm. The number of kinetic parameter involved for a particular reaction depends on the type of model chosen. Based on previous studies a sequential Mars van Krevelan (MVK) reaction model is considered for the propane ODH reaction. The MVK mechanism assumes that gas phase propane molecule reacts with lattice oxygen of the catalysts to form the primary product propene. The propene molecule further react with lattice oxygen to produce carbon oxides (CO_x = CO + CO_2). The gas phase oxygen replenishes the lattice oxygen by re-oxidation of the catalysts. The details of the kinetic modeling and kinetic parameter estimation are given elsewhere [7, 20 and ref therein]. Standard error calculations of the kinetic parameters are achieved by applying previously defined equations [20, 21].

3 Results and Discussion

3.1 Characterization of TiO_2/SiO_2 Support

The particulars of TiO_2/SiO_2 supports are tabulated as in the second to fifth row of Table 1. From these rows it is observed that an increase in titania content in TiO_2/SiO_2 supports results in a decrease in surface area. Such a decrease in surface area has been observed previously [22] and is associated with blocking of micro pores due to the building up of the titania layer in the TiO_2/SiO_2 supports. The difference in atomic weight of Si and Ti may also contribute to the decrease in surface area. The particulars

Table 1 Particulars of SiO_2 and TiO_2/SiO_2 supports and supported vanadia catalysts

Nomenclature	V_2O_5 (wt%)	Surface area (m^2/g)	Surface density (V atoms/nm^2)	T_{max} (K)	CO_2/CO[a] ψ
SiO_2	–	210			
10Ti–Si	–	203	–	–	–
30Ti–Si	–	185	–	–	–
50Ti–Si	–	159	–	–	–
70Ti–Si	–	119	–	–	–
2V30Ti–Si	2.0	170	0.8	–	0.68
2V50Ti–Si	2.0	148	0.9	712	0.74
2V70Ti–Si	2.0	110	1.2	714	0.72
4V50Ti–Si	4.0	136	2.0	727	0.52
7.5V50Ti–Si	7.5	118	4.2	744	0.44
10V50Ti–Si	10.0	103	6.4	769, 805, 840	0.43

[a] Based on entire reaction data. Standard errors are given in parenthesis. $T_m = 643.15$ K

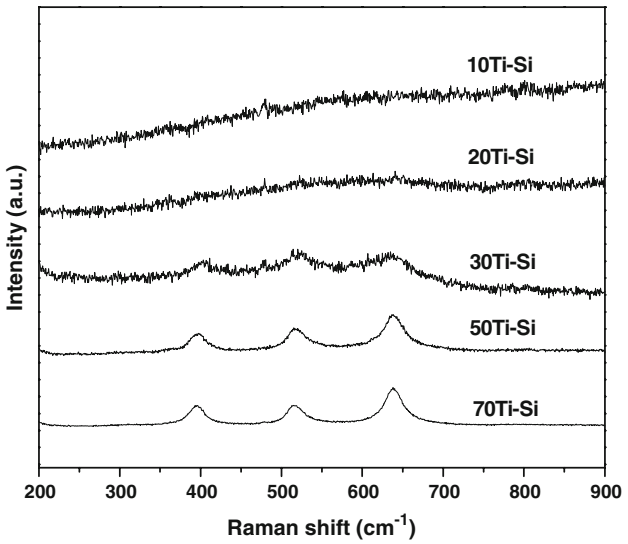

Fig. 1 Raman spectra of TiO_2/SiO_2 (xTi–Si, x = 10–70 wt%) supports obtained under ambient condition

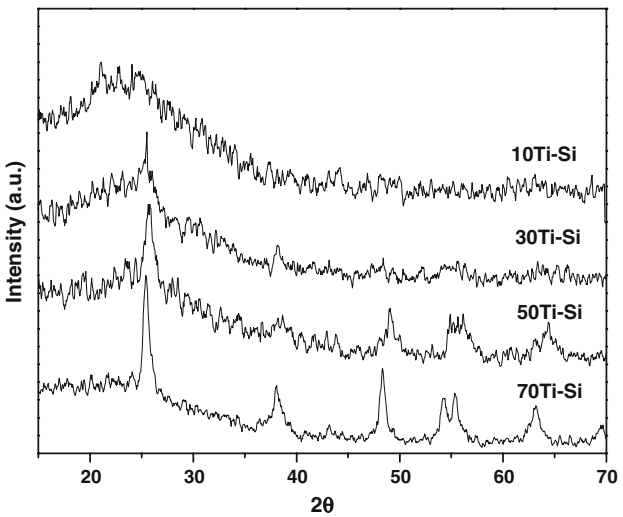

Fig. 2 XRD patterns of TiO_2/SiO_2 (xTi–Si, x = 10–70 wt%) supports calcined at 1073 K

of the vanadia supported samples are also given in Table 1 and are discussed later.

The Raman spectra of the TiO_2/SiO_2 supports of varying titania content were obtained under ambient conditions and are shown in Fig. 1. The Raman spectra in Fig. 1 reveal the presence of bulk anatase titania in the anatase phase above 30 wt% titania and the intensity of bulk anatase titania peaks increase with an increase in titania content. At 30 wt% titania, weak features of bulk anatase titania are observed. These results suggest that titania is dispersed in the TiO_2/SiO_2 samples below 30 wt% titania and bulk anatase titania is present in addition to dispersed titania above 30 wt% titania. Thus, the monolayer loading of titania on this SiO_2 support is $\sim$30 wt%, which corresponds to $\sim$12.2 Ti atoms/nm^2.

The XRD patterns of the TiO_2/SiO_2 supports were obtained and are shown in Fig. 2. The XRD patterns are shown as a function of titania content in the TiO_2/SiO_2 supports calcined at 1073 K. At 723 K calcination temperature the XRD patterns are similar to those shown in Fig. 2 (Included as Supplementary Figure S1 for review purposes only). The XRD patterns of the TiO_2/SiO_2 supports reveal no bulk titania features at and below 30 wt% of titania, which suggest that titania is well dispersed. Above 30 wt% titania bulk anatase TiO_2 phase is present, which corroborates the findings of the Raman studies given in Fig. 1. Similar results have been reported earlier where detailed studies revealed the presence of dispersed TiO_x species below monolayer coverage [23]. Interestingly, no anatase to rutile phase transformation is observed at these high calcination temperatures (1073 K) even for the 50Ti–Si and 70Ti–Si supports. In comparison, commercially available titania (Degussa P25) undergoes complete anatase to rutile phase transformation at 973 K (Included as

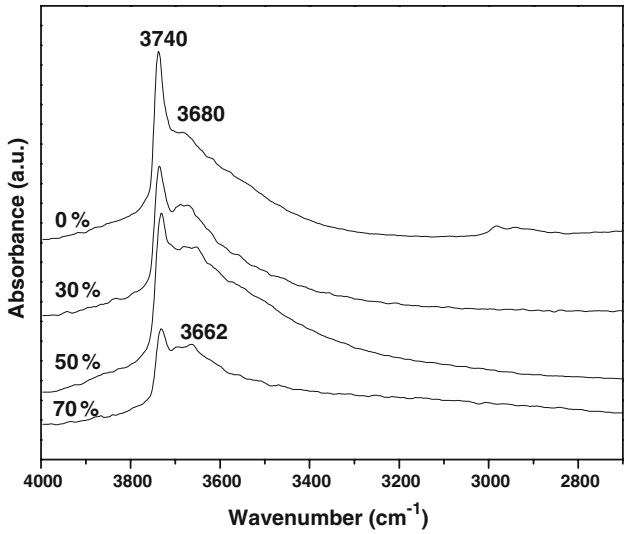

Fig. 3 Dehydrated FTIR spectra of $xTiO_2/SiO_2$ (x = 0–70 wt%) in hydroxyl region

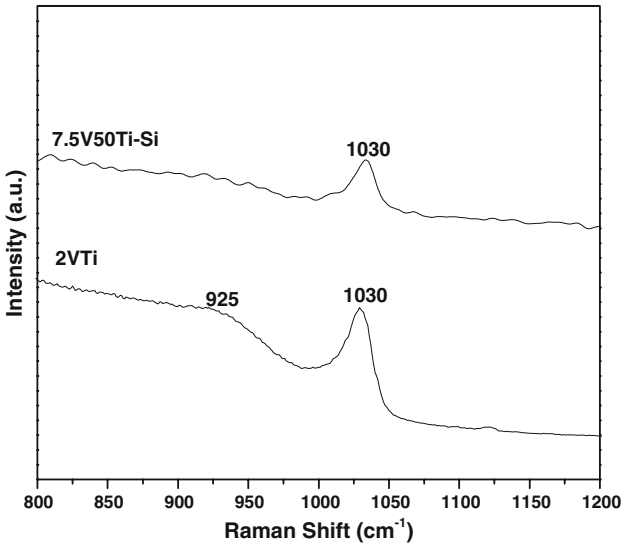

Fig. 4 Raman spectra of 2VTi and 7.5V50Ti–Si catalysts obtained under dehydrated condition

Supplementary Figure S2 for review purposes only). The results of the present study suggest that the anatase phase of titania does not undergo phase transformation when anchored to the silica support for calcinations temperatures up to 1073 K.

The dehydrated FTIR spectra of the TiO_2/SiO_2 supports were also obtained. The dehydrated IR spectra in the low wavenumber region are dominated by silica features and any additional bands are not readily observed. Changes in the IR spectra of the TiO_2/SiO_2 supports in the 2700–4000 cm^{-1} hydroxyl region are, however, observed and are shown in Fig. 3. The dehydrated IR spectrum of pure SiO_2 support reveals two bands at 3740 and 3680 cm^{-1}, which are assigned to the isolated Si–OH hydroxyl bond and the hydrogen bonded hydroxyl group vibrations, respectively [24–26]. The 3740 cm^{-1} band intensity of SiO_2 decreases as the amount of TiO_2 increases in the TiO_2/SiO_2 support suggesting the partial removal of isolated hydroxyl groups of the SiO_2 support. A weak band at 3662 cm^{-1} appears at 50 wt% titania and above, which has been assigned to the isolated Ti–OH hydroxyl bond vibration [24–26]. Raman studies, as reported above, confirmed the presence of well defined bulk titania at 50 wt% TiO_2 and above suggesting that the Ti–OH hydroxyls are associated with the bulk TiO_2 phase formed.

3.2 Characterization of Supported Vanadia Catalysts

The particulars of supported vanadia catalysts are also tabulated as in rows 6–12 in Table 1. For a specific TiO_2/SiO_2 support a decrease in surface area with an increase in vanadia loading is observed, see for example the yV50Ti–Si samples. The decrease in surface area with an increase in loading is attributed to the blocking of micro-pores. The difference in atomic weight of Si, Ti and V may also contribute to the loss in surface area since the surface area is presented with respect to gram of sample.

The Raman spectra of the four yV50Ti–Si catalysts, y = 2, 4, 7.5 and 10, were also obtained under both ambient and dehydrated condition. Two representative Raman spectra obtained under dehydrated conditions are shown in Fig. 4. A Raman band is observed at 1030 cm^{-1} due to the terminal V=O bond vibration of the molecularly dispersed vanadia species on the 50Ti–Si support [14, 27, 28]. Raman spectra of the other yV50Ti–Si catalysts reveal features due to molecularly dispersed vanadia species below 10 wt% vanadia loading. For the 10V50Ti–Si sample a Raman band at 998 cm^{-1} is observed, which is assigned to bulk V_2O_5 [6, 29], and suggests that monolayer coverage has been exceeding on the 50Ti–Si support.

The four yV50Ti–Si catalysts were also characterized by FTIR spectroscopy under dehydrated condition. The FTIR spectra of 50Ti–Si and yV50Ti–Si in the hydroxyl region are shown in Fig. 5. The FTIR spectrum of 50Ti–Si and yV50Ti–Si reveal two bands at 3732 and 3662 cm^{-1}. As mentioned above, the IR band at 3732 cm^{-1} is assigned to isolated Si–OH vibrations and the band at 3662 cm^{-1} is assigned to isolated Ti–OH vibrations. The gradual disappearance of both surface hydroxyl groups is observed upon addition of vanadium oxide. However, the relative titration of one hydroxyl species over the other is not evident since it appears that the Si–OH and Ti–OH vibrations both decrease when the vanadia loading is increased. These results suggest that the vanadia species anchor to the TiO_2/SiO_2 support by titrating the surface Si–OH and Ti–OH hydroxyl groups.

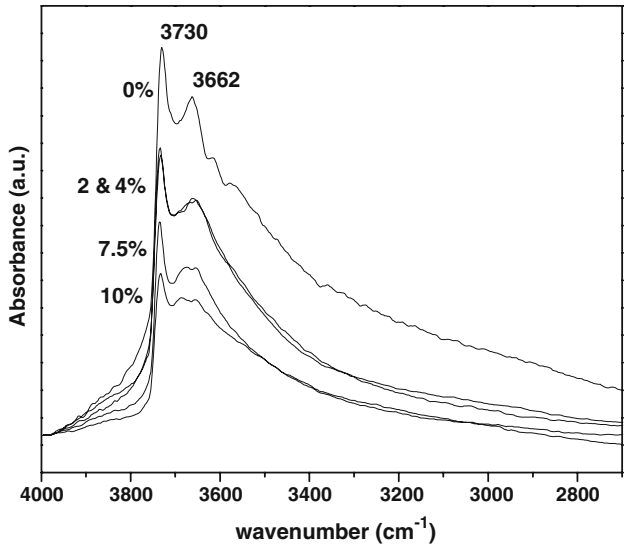

Fig. 5 Dehydrated FTIR spectra of yV50Ti–Si (y = 0–10 wt%) in hydroxyl region

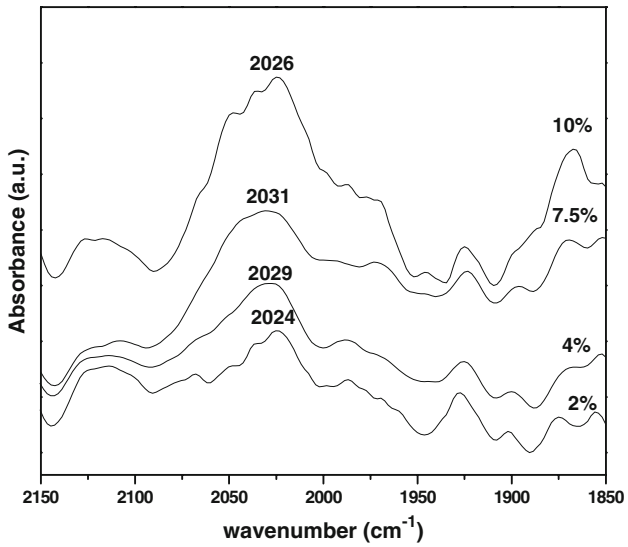

Fig. 6 Dehydrated FTIR spectra of yV50Ti–Si (y = 2–10 wt%). Background quantitatively subtracted

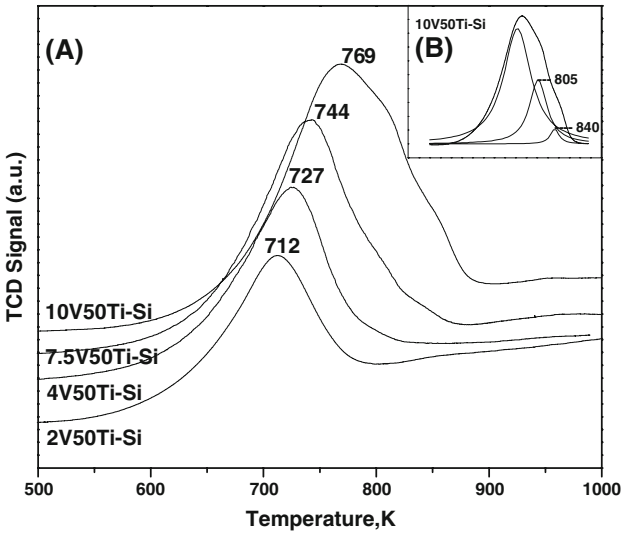

Fig. 7 TPR profile of (**a**) yV50Ti–Si (y = 2–10 wt%) and (**b**) 10V50Ti–Si after deconvolution

The dehydrated FTIR spectra in the low wavenumber region for the four yV50Ti–Si catalysts are dominated by silica features. To obtain information of the surface vanadia species, the spectra of the 50Ti–Si support is quantitatively subtracted from the spectra of the 50Ti–Si supported vanadia catalysts, and are shown in Fig. 6. After subtraction, an overtone band at ~2030 cm^{-1} is observed for all vanadia loadings. The ~2030 cm^{-1} band is due to the V=O terminal bond overtone vibration of the surface vanadia species [30]. The ~2030 cm^{-1} band is also observed in the TiO_2 (P-25) supported vanadia catalysts of the present study and is shown later. It appears that the V=O overtone band intensity increases with an increase in vanadia loading suggesting an increase in the surface vanadia species concentration.

The four catalysts, yV50Ti–Si, were also characterized by H_2-TPR and the TPR profiles of these catalysts are shown in Fig. 7. Only one temperature maxima, T_{max}, was observed for the catalysts till a loading of 7.5 wt% vanadia, 7.5V50Ti–Si. For the 10V50Ti–Si sample additional reduction features at 805 and 840 K were observed and are shown in the insert of Fig. 9. The T_{max} values of the yV50Ti–Si catalysts are tabulated in the last column of Table 1 and it is observed that the T_{max} values for the yV50Ti–Si catalysts increase from 712 to 769 K as the vanadia loading is increased. In comparison, the T_{max} values for the VTi (1–6% V_2O_5) catalysts varies from 685 to 725 K [30] and for the SiO_2 supported vanadia samples, VSi (1–7% V_2O_5), varies from 774 to 814 K [31] (Included as Supplementary Figure S3 for review purposes only). Additionally, for the higher loading VSi samples, two reduction peaks were observed: one at 814 and the other at ~850 K. TPR studies of a physical mixture of V_2O_5 and SiO_2, 3 and 5 wt% V_2O_5 + SiO_2 samples, were also carried out and two reduction peaks at ~868 and ~950 K were observed. Thus, the ~840 K shoulder observed for the 10V50Ti–Si samples appears to be due to the reduction of bulk V_2O_5, which is consistent with the Raman studies. Furthermore, the ~805 K shoulder in the reduction profile of 10V50Ti–Si appears to be due to the reduction of the surface vanadia species not associated with the bulk titania phase. These results suggest that part of the surface vanadia species is present on the exposed silica support and may be associated with the molecularly dispersed surface titania phase present on this sample. The presences of the surface vanadia species on the silica support for the other yV50Ti–Si

samples are, however, not clear. These characterization studies reveal that the surface vanadia species has a "titania" or "silica" like character depending on the vanadia loading on a specific TiO_2/SiO_2 support. At low vanadia loading on the 50Ti–Si support the surface vanadia species is present on the titania part of the support, where as for high vanadia loadings, some surface vanadia species is predominantly present on the titania part of the oxide support and the remaining surface vanadia species is present on the silica part of the support.

3.3 Ethane and Propane ODH of the Supported Vanadia Catalysts

The ethane and propane ODH reaction was carried out as a function of contact time at a particular alkane to oxygen ratio and reaction temperature. The ethane and propane conversion were observed to increase with an increase in contact time for all catalysts. Based on the reaction data the alkane conversion versus alkene yield is plotted in Figs. 8 and 9a, b. Two specific types of variations are observed in these figures: variation with respect to the titania content for the same vanadia loading, Fig. 8, and variation with respect to the vanadia content for the same TiO_2/SiO_2 support, Fig. 9a, b. From these figures it is observed that at the same alkane conversion value:

$$2V30Ti-Si < 2V50Ti-Si \leq 2V70Ti-Si \text{ and}$$
$$2V50Ti-Si < 4V50Ti-Si < 7.5V50Ti-Si \approx 10V50Ti-Si$$

Thus, for the same vanadia loading (2VxTi–Si) the alkene yield increases with an increase in titania content till bulk titania phase is well-formed and for the same titania

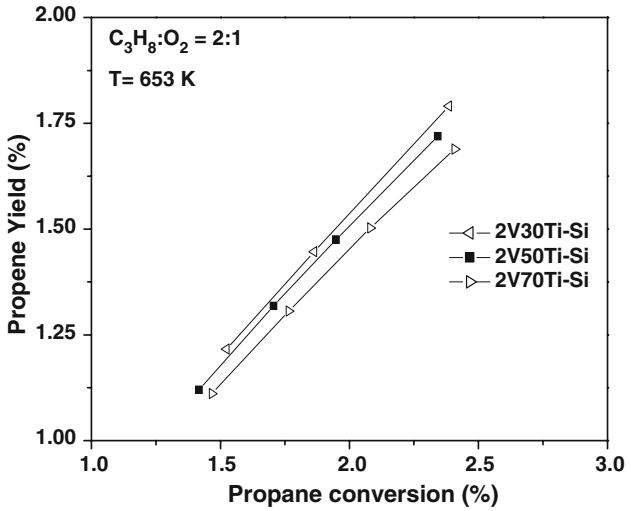

Fig. 8 Variation of propane conversion (%) versus propene yield (%) for 2VxTi–Si catalysts. T = 653 K, C_3H_8:O_2 = 2:1

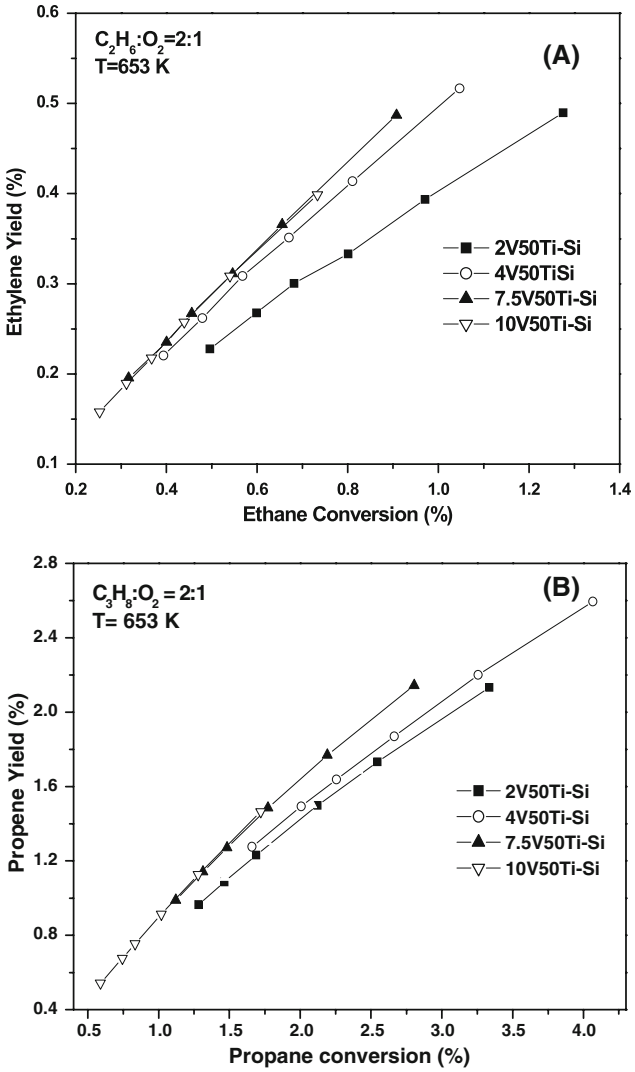

Fig. 9 Variation of (**a**) ethane conversion (%) versus ethylene yield (%) and (**b**) propane conversion (%) versus propene yield (%) for yVxTi–Si catalysts. T = 653 K, C_3H_8:O_2 = 2:1

content in the support (yV50Ti–Si) the activity increases till 7.5V50Ti–Si and is then relatively constant for the 10V50Ti–Si catalyst. The relatively constant alkene yield of the 10V50Ti–Si catalyst is due to the presence of less active bulk V_2O_5, which is detected by the Raman and TPR studies. Thus, the titania content of the support and vanadia content in the supported phase are important factors to consider while making a suitable TiO_2/SiO_2 supported vanadia catalyst.

Further understanding of the catalysts is possible by analyzing the kinetic parameters. The kinetic parameters associated with the propane ODH reaction for the six catalysts are estimated and presented in Table 2. A sequential MVK reaction model for the propane ODH reaction is considered in the present study and has been described previously [7]. The values of CO_2/CO ratio, ψ, used in

Table 2 Kinetic parameter values of the TiO_2/SiO_2 supported vanadia catalysts

Parameter	Units	Catalysts					
		2V30Ti–Si	2V50Ti–Si	2V70Ti–Si	4V50Ti–Si	7.5V50Ti–Si	10V50Ti–Si
k_{10}	mL STP min^{-1} (g cat)$^{-1}$ atm^{-1}	22 (0.2)	44 (0.01)	42 (0.3)	67 (0.02)	113 (0.03)	108 (0.05)
k_{20}		549 (10)	934 (0.01)	821 (10)	1204 (0.5)	1567 (1)	1384 (1)
k_{30}		526 (7)	324 (0.5)	296 (4)	636 (1)	1269 (1)	411 (0.2)
k_{10}/k_{20}	–	0.04	0.05	0.05	0.06	0.07	0.08
E_1	kJ mol^{-1}	92 (1)	71 (1)	65 (1)	72 (1)	69 (1)	57 (1)
E_2		44 (1)	46 (1)	49 (2)	47 (1)	54 (1)	47 (1)
E_3		83 (2)	155 (1)	143 (2)	134 (1)	133 (1)	110 (1)
$E_1 - E_2$		48	25	16	25	15	10

Standard errors are given in parenthesis. $T_m = 643.15$ K

kinetic parameter estimation are shown in Table 1. The values of ψ decreases as vanadia loading is increased, whereas ψ is relatively constant for different titania content in the TiO_2/SiO_2 supported catalysts. Along with the kinetic parameters, k_{i0}'s and E_i's, and their units, the standard error associated with each kinetic parameter are also calculated and are shown in Table 2. Comparison of standard errors with parameter values suggest that the kinetic parameter values are estimated with reasonable degree of accuracy. Moreover, a comparison between the actual and predicted concentration of all compounds analyzed reveal that a close correspondence exists and are not shown here for brevity (Included as Supplementary Figure S4 for review purposes only).

Analysis of kinetic parameter given in Table 2 reveals that variation of the different parameters follows certain trends. For 2 wt% vanadia loading the pre-exponential factors and activation energies are different for the TiO_2/SiO_2 support containing dispersed titania, 2V30Ti–Si, and the TiO_2/SiO_2 support containing bulk anatase titania, 2V50Ti–Si and 2V70Ti–Si. It appears that for the 2V30Ti–Si catalyst the surface vanadia phase is associated with the dispersed titania phase [32] and the propane ODH activity and kinetic parameters are different. In contrast, for the 2V50Ti–Si and 2V70Ti–Si samples bulk titania is present in the TiO_2/SiO_2 support and the surface vanadia species is able to anchor preferentially onto the bulk titania phase of the TiO_2/SiO_2 support. Consequently, the propane ODH activity and kinetic parameters are similar for 2V50Ti–Si and 2V70Ti–Si catalysts.

The kinetic parameter values for the different vanadia loadings supported on the same TiO_2/SiO_2 support, yV50Ti–Si samples, reveals that with an increase in vanadia loading the k_{10}, k_{20} and k_{30} values increase till 7.5 wt% vanadia after which the pre-exponential factors decrease for the 10V50Ti–Si catalyst. As mentioned above, the 10V50Ti–Si catalyst possesses bulk V_2O_5, which are detrimental for the propane ODH reaction [29]. The activation energies for the 2V50Ti–Si, 4V50Ti–Si and 7.5V50Ti–Si catalysts are similar but decrease for the 10V50Ti–Si sample, which again may be associated with the presence of the bulk V_2O_5 phase.

In order to understand the effect of different TiO_2/SiO_2 supported catalysts on the propene yield at iso-conversion the lumped parameter k_1/k_2 is important to analyze [7, 21, 29]. The importance of the lumped parameter arises since for a series reaction the propene yield at iso-conversion depends on the ratio of rate constants, k_1/k_2 [33]. The k_1/k_2 ratio for various catalysts in turn depends on the value of k_{10}/k_{20} and difference in activation energies, $E_1 - E_2$. The k_{10}/k_{20} value is the k_1/k_2 value at $T = T_m$, where T_m is the mean reaction temperature. The values of k_{10}/k_{20} and $E_1 - E_2$ are also given in Table 2 along with the kinetic parameter. It is observed that the k_{10}/k_{20} value is: (i) similar for the 2V50Ti–Si and 2V70Ti–Si catalysts, where the surface vanadia species is associated with the bulk titania phase and (ii) larger than the 2V30Ti–Si catalysts, where the surface vanadia species is associated with the silica support with or without dispersed titania in it vicinity. Furthermore, for the yV50Ti–Si samples, increasing the vanadia content increases the k_{10}/k_{20} ratio similar to those observed for pure TiO_2 supported vanadia catalysts, xVTi [7].

At reaction temperatures different from T_m the k_1/k_2 ratio would depend on the value of $E_1 - E_2$. For all catalysts it is observed that $E_1 - E_2$ is positive, which implies that the k_1/k_2 ratio increases with temperature and, consequently, the propene yield at iso-conversion also increases with temperature. The rate of increase in k_1/k_2 ratio with temperature would depend on the magnitude of $E_1 - E_2$. A larger $E_1 - E_2$ value would indicate a more rapid increase of the k_1/k_2 value. With an increase in titania content in the TiO_2/SiO_2 support for the 2 wt% vanadia catalysts, 2VxTi–Si, the $E_1 - E_2$ value decreases resulting in a decrease in the rate of increase of k_1/k_2. Furthermore, for the same TiO_2/SiO_2 support used to make the catalysts, yV50Ti–Si,

increasing the vanadia content results in the $E_1 - E_2$ value to be initially constant and then decrease. This variation in $E_1 - E_2$ is due to the initial constant values of E_1 and E_2 and then the decrease in E_1 value and increase in E_2 value. Despite the specific variations in the $E_1 - E_2$ value for the different catalysts the major trends observed for the variation of k_{10}/k_{20} for the different catalysts still hold for the variations of k_1/k_2 for the different catalysts. Thus, the propene yield at iso-conversion values: increases with temperature for all catalysts, is higher for the TiO_2/SiO_2 support possessing bulk titania phase for catalysts possessing the same vanadia content; increases with an increase in vanadia content for the same TiO_2/SiO_2 support, 50Ti–Si.

3.4 Effect of Catalyst Calcination Temperature

To see the effect of calcination temperature the surface area of 2VTi, 4VTi, 2V50Ti–Si and 4V50Ti–Si calcined in the temperature range 723–1073 K were also determined. It is observed that the surface area decreases as the calcination temperature is increased for the all above mentioned samples. Similar decreasing trends in surface area with an increase in calcination temperature for TiO_2 (Degussa P25) was also reported earlier [34]. To observe specific changes with calcination temperatures the surface areas are normalized with respect to the initial surface areas of the samples and are shown in Fig. 10 for 4VTi and 4V50Ti–Si catalysts. It is clear from Fig. 10 that the decrease in surface area with an increase in calcination temperature of TiO_2 (Degussa P25) supported catalysts, 4VTi, is more rapid than the TiO_2/SiO_2 supported vanadia catalysts, 4V50Ti–Si. Specifically, the 4V50Ti–Si catalyst retains it surface area till 773 K and then continuously decreases, whereas the surface area of the 4VTi sample decreases continuously and more rapidly. It is also observed that the rate of decrease in surface area with temperature is a function of vanadia loading. Such a decrease in surface area may be attributed to the change in pore structure due to sintering with temperature and/or phase transformations as discussed later.

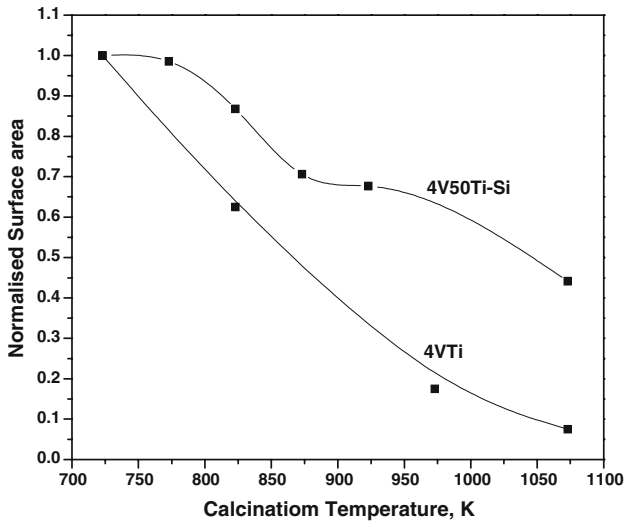

Fig. 10 Variation of normalized surface area with calcination temperature for 4VTi and 4V50Ti–Si catalysts

The yV50Ti–Si catalysts were calcined at different temperatures and characterized by XRD to determine phase changes in the support. The XRD patterns at 723 K revealed features of the anatase phase only for the yV50Ti–Si samples. At higher temperatures, depending on the sample, the anatase phase transformation occurs for the TiO_2/SiO_2 supported vanadia samples. No anatase to rutile phase transition was observed for the 2V50Ti–Si catalyst sample even at a calcination temperature of 1073 K, whereas the rutile phase appeared at a calcination temperature of: 973 K for the 4V50Ti–Si catalyst and 7.5V50Ti–Si catalysts. Furthermore, the anatase to rutile phase transformation is: not complete even at 1073 K for 4V50Ti–Si catalyst and is complete at 1073 K for the 7.5V50Ti–Si catalyst (Included as Supplementary Figure S5 for review purposes only). In contrast the complete anatase to rutile phase transformation for 4VTi catalyst was observed at a calcination temperature of 923 K. None of the XRD patterns are shown here for brevity. These results suggest that the anatase phase in the TiO_2/SiO_2 supports and the TiO_2/SiO_2 supported vanadia catalysts are unaffected at high calcinations temperatures compared to titania (Degussa P25) supported vanadia catalysts. Furthermore, the anatase to rutile phase transformation takes place at lower temperatures when vanadia is present and the phase transformation temperature further decreases with an increase in vanadia loading. It appears that surface vanadia species catalyzes the anatase to rutile phase transformation. Previous studies on pure TiO_2 supported vanadia samples suggest that during anatase to rutile phase transformation part of the vanadia species is reduced to V^{+4} and is incorporated in the rutile matrix to form a solid solution of general formulae $V_xTi_{(1-x)}O_2$ [35–37].

The effect of calcinations temperature on TiO_2/SiO_2 supported vanadia catalysts, yVxTi–Si, for the alkane ODH reaction were tested by calcining the catalysts at different temperatures and observing the changes, if any, of the catalytic activity. These result were compared with TiO_2 (Degussa P25) supported vanadia catalysts, xVTi. In the present study the propane ODH reaction was carried out over some representative catalysts, 2VTi, 4VTi, 2V50Ti–Si and 4V50Ti–Si, calcined at different temperature (723–1073 K). The propane ODH reaction was carried out at 673 K, propane to oxygen to nitrogen molar ratio of

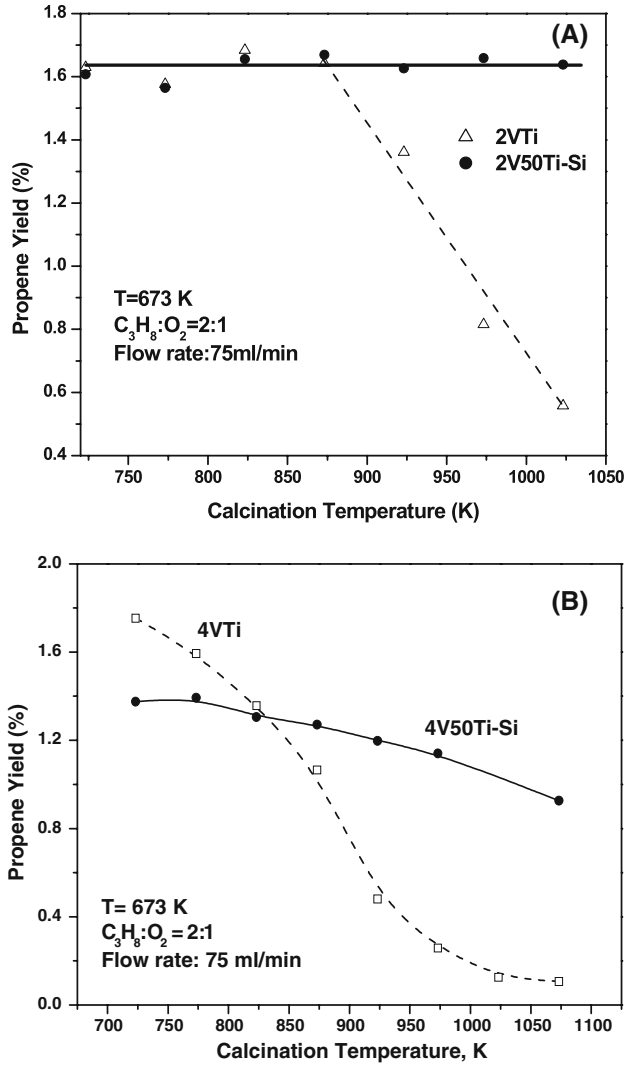

Fig. 11 Variation of propene yield with calcination temperature for (**a**) 2VTi and 2V50Ti–Si catalysts and (**b**) 4VTi and 4V50Ti–Si catalysts

2:1:3.8, and a total flow rate of 75 mL/min. The propene yield as a function of calcination temperature for 2VTi and 2V50Ti–Si is shown in Fig. 11a and for 4VTi and 4V50Ti–Si in Fig. 11b. The catalysts considered in Fig. 11a, b possess the same amount of vanadia per gram catalyst. For the 2VTi catalyst the propene yield is initially constant and then decreases at high calcination temperatures suggesting the expected high temperature deactivation of the catalyst, whereas for the 2V50Ti–Si catalyst no variation in propene yield is observed with an increase in calcination temperature up to 1073 K. Hence, for this vanadia loading the 50Ti–Si supported vanadia catalyst does provide lower deactivation in terms of maintaining the propane ODH activity up to high calcination temperature. It is expected that the 2V50Ti–Si can be used for high temperature reactions without the catalyst deactivating during reaction.

In contrast, the propene yield for 4VTi continuously decreases with an increase in calcination temperature and for 4V50Ti–Si the yield is constant till 773 K and then decrease with an increase in calcination temperature. The propene yield for 4VTi is initially higher, decreases more rapidly and is finally lower than 4V50Ti–Si. Consequently, a limited effect of calcinations temperature is available for this vanadia loading on the 50Ti–Si support. The higher activity of 4VTi compared to 4V50Ti–Si at low calcination temperatures may be due to part of the surface vanadia species being present on the silica support rather than the more active bulk titania phase of the 50Ti-Si support.

The effect on the vanadia active sites with calcinations temperature for the 4VTi catalyst was undertaken by studying the changes in the IR spectra. The spectra of the 4VTi catalysts at different calcinations temperatures are given in Fig. 12. As observed in Fig. 12, the concentration of surface vanadia species, indicated by the $\sim$2030 cm^{-1} band, decreases with an increase in calcination temperature for 4VTi catalyst suggesting that the loss of ODH activity with increase in calcination temperatures is due to the loss of the surface vanadia species. The surface areas of 4VTi and 4V50Ti–Si catalysts calcined at various temperatures also reveal that the surface area of 4VTi decreases more rapidly than 4V50Ti–Si with calcination temperature as discussed above. Furthermore, the XRD pattern of these catalysts at different calcination temperatures reveal that anatase to rutile phase transformation is accelerated in the presence of vanadia. These results suggest that the loss of activity with increase in calcination temperature is associated with a loss of surface active vanadia sites, which is accompanied by two processes occurring independently: anatase to rutile phase transformation and loss of surface area.

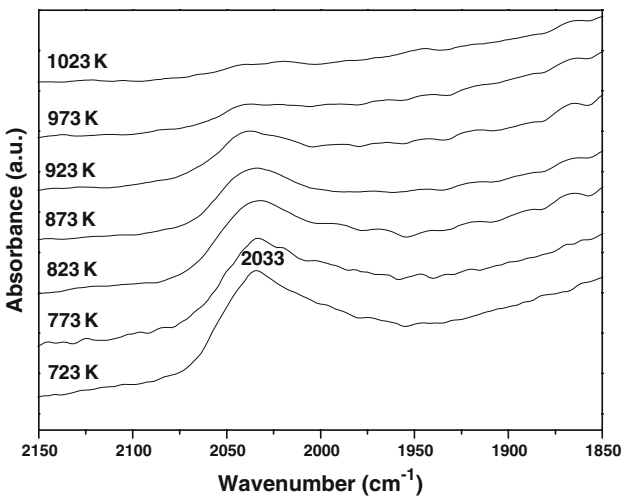

Fig. 12 Dehydrated FTIR spectra of 4VTi calcined at different temperature

4 Conclusions

Several TiO_2/SiO_2 supports were synthesized by the incipient wetness impregnation method to obtain relatively high surface area titania-based support that is not affected by high temperatures. Vanadia supported on these TiO_2/SiO_2 supports were also synthesized by the same method. It was observed that the surface area decreases as: the titania loading is increased in the TiO_2/SiO_2 support and vanadia loading is increased in the supported vanadia catalysts. The Raman spectra and XRD studies reveal that the monolayer coverage of titania on silica is achieved at $\sim$12.2 Ti atoms/nm^2. Below monolayer coverage titania is predominately present as a dispersed phase and above monolayer coverage bulk anatase titania is present in addition to the dispersed phase. The XRD patterns of various TiO_2/SiO_2 supports reveal that the anatase to rutile transformation does not occur up to 1073 K. The phase transformation, however, is favored by the presence of surface vanadia. The surface area of TiO_2 (Degussa P25) supported vanadia catalysts was observed to decreases more rapidly than the TiO_2/SiO_2 supported vanadia catalysts. Dehydrated FTIR spectra of supported vanadia catalysts calcined at high temperature also revealed that the amount of surface vanadia species decrease as the calcination temperature increased. The H_2-TPR studies demonstrated that at low vanadia loading the surface vanadia species anchors preferably on titania and at high vanadia loadings the surface vanadia species also anchor on expose SiO_2.

The ethane and propane ODH studies reveal that propane conversion is a function of titania content in TiO_2/SiO_2 and vanadia loading. Analysis of the TiO_2/SiO_2 supported vanadia catalysts for propane ODH reaction was also achieved by studying the kinetic parameter variations. Analysis of reaction data reveals that the values of different kinetic parameters correlate well with different vanadia species anchored on titania and exposed silica in the TiO_2/SiO_2 support. At similar vanadia loading, the kinetic parameters values for low titania containing TiO_2/SiO_2 supported catalysts are different from high titania containing TiO_2/SiO_2 supported catalyst. For low titania containing TiO_2/SiO_2 supports it appears that the surface vanadia species are anchored to the support that may or may not possess dispersed titania in its vicinity. For higher titania containing TiO_2/SiO_2 supported catalysts, the activity and kinetic parameter values are similar to those of TiO_2 (Degussa P25) supported vanadia catalysts for low loadings, 2 wt%. At high vanadia loading, however, the activity values are lower than the TiO_2 (Degussa P25) supported vanadia catalyst of similar loading. The lower activity for these TiO_2/SiO_2 supported vanadia catalysts appears to be due to the anchoring of part of the surface vanadia species on the silica exposed surface which may or may not have dispersed titania in its vicinity. The ODH activity results also reveal the effect of calcinations temperature on the TiO_2/SiO_2 supported catalysts (yV50Ti–Si). Depending on the vanadia loading the activity at higher calcination temperature is retained or decreases less rapidly when compared to the pure titania supported catalysts (xVTi). The disadvantage of using the TiO_2/SiO_2 support is that for high vanadia loadings part of the surface vanadia species may be present on the exposed silica part of the support that may or may not possess the dispersed titania species in its vicinity. Thus, the efficient design of TiO_2/SiO_2 supported vanadia catalysts possessing high surface area and maintaining the ODH activity to high calcinations temperatures involves knowledge of the titania and vanadia content of the catalysts.

Acknowledgment The authors are thankful to Prof. Israel E. Wachs, Lehigh University, for providing the Raman spectra. The authors gratefully acknowledge the support from the Department of Science and Technology (DST), India.

References

1. Mamedov EA, Corberan VC (1995) Appl Catal A: Gen 127:1
2. Deo G, Wachs IE, Haber J (1994) Crit Rev Surf Chem 4:141
3. Sanati M, Anderson A (1991) Ind Eng Chem Res 30:320
4. Wachs IE, Saleh RY, Chan SS, Cherish CC (1985) Appl Catal 15:339
5. Bond GC, Bruckman K (1982) Faraday Discuss Chem Soc 72:235
6. Routray K, Reddy KRSK, Deo G (2004) Appl Catal A: Gen 265:103
7. Shee D, Rao TVM, Deo G (2006) Catal Today 118:288
8. Miller JB, Ko EI (1997) Catal Today 35:269
9. Gao X, Bare SR, Fierro JLG, Bañares MA, Wachs IE (1998) Phy Chem B 102:5653
10. Reddy BM, Ganesh I, Chowdhury B (1999) Catal Today 49:115
11. Handy BE, Baiker A, Marth MS, Wokaun A (1992) J Catal 133:1
12. Reiche MA, Ortelli E, Baiker A (1999) Appl Catal B: Environ 23:187
13. Santacesaria E, Sorrentino A, Tessr A, Di Serio M, Ruggiero A (2003) J Mol Catal A: Chem 204–205:617
14. Khodakov A, Olthof B, Bell AT, Iglesia E (1999) J Catal 181:205
15. Lemonidou AA, Nalbandian L, Vasalos IA (2000) Catal Today 61:333
16. Matra G, Arena F, Coluccia S, Frusteri AP (2000) Catal Today 63:197
17. Wachs IE, Weckhuysen BM (1997) Appl Catal A: Gen 157:67
18. Poelman H, Sels BF, Olea M, Eufinger K, Paul JS, Moens B, Sack I, Balcan V, Bertinchamps F, Gaigneaux EM, Jacobs PA, Marinc GB, Poelmana D, De Grysea R (2007) J Catal 245:156
19. Mitra B, Wachs IE, Deo G (2006) J Catal 240:151
20. Routray K, Deo G (2005) J AIChE 51:1733
21. Singh RP, Bañares MA, Deo G (2005) J Catal 233:388
22. Wauthoz P, Ruwet M, Machej T, Grange P (1991) Appl Catal 69:149
23. Quaranta NE, Soria J, Corberan VC, Fierro JLG (1997) J Catal 171:1
24. Vuurman MA, Wachs IE (1993) J Mol Catal 80:209

25. Busca G, Saussev H, Saur O, Lavalley JC, Lorenzelli V (1985) Appl Catal 14:245
26. Jackson P, Parfitt GD (1972) J Chem Soc Faraday Trans 1 68:896
27. Magg N, Immaraporn B, Giorgi JB, Schroeder T, Baumer M, Dobler J, Wu Z, Kondratenko E, Cherian M, Baerns M, Stair PC, Sauer J, Freund HJ (2004) J Catal 226:88
28. Wachs IE, Chen Y, Jehng JM, Briand LE, Tanaka T (2003) Catal Today 78:13
29. Rao TVM, Deo G (2007) Ind Eng Chem Res 46:70
30. Busca G (1988) Mater Chem Phys 19:157
31. Chakraborty S, M. Tech. Thesis (2007) I.I.T. Kanpur, India
32. Gao X, Bare SR, Fierro JLG, Wachs IE (1999) J Phys Chem B 103:618
33. Fogler HS (2002) Elements of chemical reaction engineering, 3rd edn. Prentice-Hall of India Pvt. Ltd., New Delhi
34. Nadia RC, Machado F, Santana VS (2005) Catal Today 107–108:595
35. Reddy BM, Kumar MV, Reddy P, Mehdi S (1996) Catal Lett 36:187
36. Saleh RY, Wachs IE, Chan SS, Chersich CC (1986) J Catal 98:102
37. Bond GC, Sarkany AJ, Parfitt GD (1979) J Catal 57:476